

## DNA-Induced Dimerization of Poly(ADP-ribose) Polymerase-1 Triggers Its Activation<sup>†</sup>

Emmanuelle Pion,<sup>‡</sup> G. Matthias Ullmann,<sup>||</sup> Jean-Christophe Amé,<sup>§</sup> Dominique Gérard,<sup>‡,⊥</sup> Gilbert de Murcia,<sup>§</sup> and Elisa Bombarda<sup>\*,‡,⊥</sup>

UMR 7034 du CNRS, Laboratoire de Pharmacologie et Physico-Chimie des Interactions Cellulaires et Moléculaires, Université Louis Pasteur de Strasbourg, 74, Route du Rhin, F-67401 Illkirch Cedex, France, Département Intégrité du Génome, CNRS, Ecole Supérieure de Biotechnologie de Strasbourg, Boulevard Sébastien Brant, F-67400 Illkirch, France, and Structural Biology/Bioinformatics, University of Bayreuth, Universitätsstrasse 30, BGI D-95447 Bayreuth, Germany

Received April 25, 2005; Revised Manuscript Received August 31, 2005

**ABSTRACT:** In response to DNA strand breaks in the genome of higher eukaryotes, poly(ADP-ribose)-polymerase 1 (PARP-1) catalyses the covalent attachment of ADP-ribose units from NAD<sup>+</sup> to various nuclear acceptor proteins including PARP-1 itself. This post-translational modification affecting proteins involved in chromatin architecture and in DNA repair plays a critical role in cell survival as well as in caspase-independent cell death. Although PARP-1 has been best-studied for its role in genome stability, several recent reports have demonstrated its role in the regulation of transcription. In this study, fluorescence spectroscopy and biochemical techniques are used to investigate the association of the amino-terminal DNA-binding domain of human PARP-1 (hPARP-1 DBD) with various DNA substrates, characterized by different DNA ends and sequence features (5'- or 3'-recessed end, double strands, telomeric repeats, and the palindromic sequence of a *Not I* restriction site). The correlation between the binding mode of hPARP-1 DBD to the DNA oligoduplexes and the enzymatic activation of hPARP-1 is analyzed. We show that hPARP-1 DBD binds a 5'-recessed DNA end cooperatively with a stoichiometry of two proteins per DNA molecule. In contrast, a 1:1 stoichiometry is found in the presence of a 3'-recessed end and double-strand DNA. A palindromic structure like the *Not I* restriction site is shown to induce protein dimerization and high enzymatic activation, suggesting that it can represent a recognition element for hPARP-1 in undamaged cells. Protein dimerization is found to be a requisite for high enzymatic activity. Taken together, our data allow further characterization of the features of hPARP-1 recognition in damaged cells and bring additional evidence that hPARP-1 may also play a role in undamaged cells.

Poly(ADP-ribosyl)ation is an immediate DNA damage-dependent post-translational modification of histones and other nuclear proteins that contributes to the repair of DNA in injured proliferating cells. Poly(ADP-ribose)polymerases (PARPs)<sup>1</sup> constitute a family of 18 proteins (*I*), encoded by different genes and displaying a conserved catalytic domain.

PARP-1, the founding member of this family, is a 113 kDa enzyme with three functional domains: an N-terminal DNA-binding domain (DBD), containing a two-zinc-fingers motif; a central automodification domain, containing a protein-protein interacting interface BRCT, present also in other enzymes and factors involved in the maintenance of genomic integrity (2); and a C-terminal catalytic domain involved in poly(ADP-ribose) (PAR) synthesis. PARP-1 fulfills several key functions in repairing an interruption of the sugar phosphate backbone: (i) efficient sensing of the break (3), (ii) translation and amplification of the damage signal into a post-translational modification of histones H1 and H2B leading to chromatin structure relaxation and to DNA accessibility (4), and (iii) immediate or concomitant recruitment of XRCC1 to the break (5–7). In vitro, PARP activation has been reported to be dependent on the type of DNA ends (8) and on the length of the DNA strands (9). The recognition of strand interruptions by PARP-1 and the following poly(ADP-ribosyl)ation of key proteins signal the presence of DNA damage to factors that regulate the repair of DNA interruptions (10). All the members of the PARP family share at various degrees of conservation the PARP signature: a block of 50 amino acids generally located in their C-terminus. This region is virtually unchanged from plants to humans and forms the catalytic site of the founding

<sup>†</sup> This work was supported by funds from CNRS, Association pour la Recherche Contre le Cancer, Electricité de France, Commissariat à l'Énergie Atomique, Ligue Nationale contre le Cancer, Ligue contre le Cancer Région Alsace, Association Régionale pour l'Enseignement et la Recherche Scientifique et Technologique, and Université Louis Pasteur.

\* Corresponding author. Tel: +33 (0)3 90 24 42 55. Fax: +33 (0)3 90 24 43 12. E-mail: elisa.bombarda@pharma.u-strasbg.fr.

<sup>‡</sup> Université Louis Pasteur de Strasbourg.

<sup>§</sup> Ecole Supérieure de Biotechnologie de Strasbourg.

<sup>||</sup> University of Bayreuth.

<sup>⊥</sup> Present address: UMR 7081 du CNRS, Laboratoire de Pharmacochimie de la Communication Cellulaire, Université Louis Pasteur de Strasbourg, 74 route du Rhin, F-67401 Illkirch Cedex, France.

<sup>1</sup> Abbreviations: BRCT, Breast cancer susceptibility protein, BRCA1, C-terminus; BSA, bovine serum albumin; DTT, dithiothreitol; PAR, poly(ADP-ribose); hPARP-1, human poly(ADP-ribose) polymerase 1; hPARP-1 DBD, DNA-binding domain of human poly(ADP-ribose) polymerase 1; HPLC, high-performance liquid chromatography; NAD, nicotinamide adenine dinucleotide; SDS, sodium dodecyl sulfate; TCA, trichloroacetic acid; Trp, tryptophan; XRCC1, X-ray cross-complementing factor 1.

Table 1: Nucleotide Sequences of the DNA Substrates Used in This Work

66-ds	5' AAG GGC AAG GCT GCT GTG GAC CCT GCT GTG GGC TGG AGA ACA AGG TGA TCT GCG CCC TGG TCC TGG 3'	3' TTC CCG TTC CGA CGA CAC CTG GGA CGA CAC CCG ACC TCT TGT TCC ACT AGA CGC GGG ACC AGG ACC 5'
66-5'R	5' AAG GGC AAG GCT GCT GTG GAC CCT GCT GTG GGC TGG AGA ACA AGG TGA TCT GCG CCC TGG TCC TGG 3'	3' TTC CCG TTC CGA CGA CAC CTG GGA CGA CAC CCG 5'
66-3'R	5' AAG GGC AAG GCT GCT GTG GAC CCT GCT GTG GGC TGG AGA ACA AGG TGA TCT GCG CCC TGG TCC TGG 3'	3' ACC TCT TGT TCC ACT AGA CGC GGG ACC AGG ACC 5'
60-ds NT	5' ATC AGA TAG CAT CTG TGC GGC CGC TTA GGG TTA GGG TTA GGG TTA GGG TTA GGG TTA GGG 3'	3' TAG TCT ATC GTA GAC ACG CCG GCG AAT CCC AAT CCC AAT CCC AAT CCC AAT CCC AAT CCC 5'
36-5'R NT	5' ATC AGA TAG CAT CTG TGC GGC CGC TTA GGG TTA GGG TTA GGG TTA GGG TTA GGG TTA GGG 3'	3' TAG TCT ATC GTA GAC ACG CCG GCG AAT CCC AAT CCC 5'
30-5'R NT	5' ATC AGA TAG CAT CTG TGC GGC CGC TTA GGG TTA GGG TTA GGG TTA GGG TTA GGG TTA GGG 3'	3' TAG TCT ATC GTA GAC ACG CCG GCG AAT CCC 5'
60-ds N	5' AAG GGC AAG GCT GCT GGC GGC CGC GAC CCT GCT GTG GGC TGG AGA ACA AGG TGA TCT GCG 3'	3' TTC CCG TTC CGA CGA CCG CCG GCG CTG GGA CGA CAC CCG ACC TCT TGT TCC ACT AGA CGC 5'
60-ds T	5' AAG GGC AAG GCT GCT GTG GAC CCT TTA GGG TTA GGG TTA GGG TTA GGG TTA GGG TTA GGG 3'	3' TTC CCG TTC CGA CGA CAC CTG GGA AAT CCC AAT CCC AAT CCC AAT CCC AAT CCC AAT CCC 5'
60-3'R N	5' AAG GGC AAG GCT GCT GGC GGC CGC GAC CCT GCT GTG GGC TGG AGA ACA AGG TGA TCT GCG 3'	3' CTG GGA CGA CAC CCG ACC TCT TGT TCC ACT AGA CGC 5'
60-3'R T	5' AAG GGC AAG GCT GCT GTG GAC CCT TTA GGG TTA GGG TTA GGG TTA GGG TTA GGG TTA GGG 3'	3' CCC AAT CCC AAT CCC AAT CCC AAT CCC AAT CCC AAT CCC 5'
60-5'R N	5' AAG GGC AAG GCT GCT GGC GGC CGC GAC CCT GCT GTG GGC TGG AGA ACA AGG TGA TCT GCG 3'	3' TTC CCG TTC CGA CGA CCG CCG GCG CTG GGA 5'

member PARP-1. Given the conservation of the C-terminal catalytic site among the whole PARP family, the elucidation of the DNA-binding properties of PARP-1 at the molecular level is an obligatory step not only in understanding its biological role but also in the development of activators and inhibitors raised specifically against the N-terminal nick binding function of PARP-1.

Activation of PARP-1 by DNA strand interruptions has been well-documented (11), and attempts to evaluate the relative affinities of this DNA damage-sensing enzyme for DNA strand interruptions have been done (12, 13). Nevertheless, a detailed study of the specific mechanism of interaction between PARP-1 and DNA structures in order to explain the determinants of PARP-1 activation has not been yet performed. We previously investigated the binding mechanism of the DNA-binding domains of human PARP-1 (hPARP-1 DBD) to a double-stranded oligonucleotide bearing a 5'-recessed end by monitoring tryptophan fluorescence intensity and anisotropy (13). The analysis of the binding data showed that two hPARP-1 DBD proteins bind the 5'-recessed DNA structure highly cooperatively. We proposed that this feature has an impact on hPARP-1 function by enhancing its activity, given the intermolecular nature of the automodification reaction (14).

In this work, fluorescence spectroscopy and biochemical techniques are used to determine the binding stoichiometry and the stability of the complex between hPARP-1 DBD and various DNA substrates. Furthermore, we investigate the correlation between the enzymatic activation of hPARP-1 and the binding mode of hPARP-1 DBD to the DNA oligoduplexes. Different classes of damaged DNA substrates are compared. We show that the palindromic structure of the *Not I* restriction site represents a recognition element for hPARP-1 leading to enzymatic activation. We further characterize the features of hPARP-1 recognition in damaged cells and bring additional evidence that hPARP-1 may also play a role in undamaged cells.

## MATERIALS AND METHODS

**Materials.** The hPARP-1 DBD (residues 1–234) cloned in the expression vector pTG161 (15) was overexpressed in *Escherichia coli* and affinity-purified on both Hydroxyapatite and DNA cellulose chromatography columns as previously described (16). Homogeneity of hPARP-1 DBD was ascertained by its relative molecular mass using 10% SDS-PAGE. The protein was stored at  $-80^{\circ}\text{C}$  in 20% glycerol. The hPARP-1 DBD concentration was determined on a Cary 400 spectrophotometer using an extinction coefficient of  $30\,620\text{ M}^{-1}\text{ cm}^{-1}$  at 280 nm. The DNA-binding buffer was 50 mM Tris-HCl, 100 mM NaCl, and 1 mM DTT, pH 8, if not otherwise stated. Oligonucleotides containing various sequences (Table 1 and Figure 1B) were synthesized at a  $0.2\ \mu\text{mol}$  scale by IBA GmbH Nucleic Acids Product Supply (Göttingen, Germany) and purified by reverse-phase HPLC and polyacrylamide gel electrophoresis by the manufacturer. Oligonucleotides concentrations were calculated at 260 nm using extinction coefficients of “G” strand and “C” strand, respectively. Annealing reactions were carried out by incubating the oligonucleotides for 2.5 min at  $85^{\circ}\text{C}$  in 50 mM Tris-HCl, pH 8.0, 300 mM NaCl, and 1 mM DTT, and then allowing them to cool slowly.

**5'-End  $\gamma$ - $^{32}\text{P}$ -Radiolabeling of Oligonucleotides.** Unlabeled oligonucleotide ( $50\ \mu\text{L}$ ) in T4 polynucleotide kinase buffer was incubated with 200 pmol of  $[\gamma$ - $^{32}\text{P}]\text{ATP}$  in the presence of T4 polynucleotide kinase for 30 min at  $37^{\circ}\text{C}$ . Then, annealing reactions were carried out by incubating the labeled oligonucleotide with the complementary sequence from  $90^{\circ}\text{C}$  to room temperature overnight. The products were purified by ethanol followed by a 10% nondenaturing polyacrylamide gel (19:1) electrophoresis buffered with Tris-Borate-EDTA (TBE). The band of gel containing the double-strand DNA was eluted by diffusion in a solution containing 50% phenol and 50% Tris-EDTA (TE) buffer overnight at  $4^{\circ}\text{C}$ . The DNA was then precipitated, and the

amount was determined by measuring the optical density at 260 nm.

**DNase I Footprinting.** Purified hPARP-1 DBD (100 ng) was immobilized onto nitrocellulose (BAS 83, Schleicher & Schuell) and allowed to bind to 20 ng of  $^{32}\text{P}$  5'-end labeled DNA at 0 °C in the binding buffer (50 mM Tris-HCl, pH 8, 150 mM NaCl, and 0.1% Nonidet P-40). Following a 1 h incubation, the membranes were washed three times with the binding buffer at 0 °C. The membranes were then either dried and subjected to autoradiography to visualize the protein–DNA complexes or autoradiographed while wet for 1 h so that the filter-bound protein–DNA complexes could be excised and used for DNase I footprinting assays as described previously (17).

**PARP Activity Assay.** The PARP activity assay was performed as described previously (18). Samples corresponding to 200 ng of PARP-1 protein were incubated for 15 min at 25 °C in assay buffer (0.1 mL) consisting of 50 mM Tris-HCl, pH 8, 2 mM  $\text{MgCl}_2$ , 150 mM NaCl, 2 mM DTT, 1  $\mu\text{g}/\mu\text{L}$  BSA, 400  $\mu\text{M}$  NAD, [ $\alpha$ - $^{32}\text{P}$ ]NAD $^{+}$ , and various oligonucleotides (200 ng). These conditions allow to be in the linear part of the kinetic curve of the enzymatic reaction (the loss of linearity occurs after 20–25 min) and ensure the highest possible processing turnover (the Michaelis–Menten constant of hPARP-1 for NAD is about 40  $\mu\text{M}$ ). The reaction was stopped by addition of 5% TCA, and the radioactivity of the TCA-insoluble material was determined on Whatman GF/C glass filters (19).

**Not I Digestion.** The protective effect of hPARP-1 DBD on DNA was observed using the action of the restriction enzyme *Not I*. The DNA substrate (5 nM) 60-ds NT, radioactively labeled as described above, was incubated with the restriction enzyme *Not I* in the presence or in the absence of 2.5 nM of hPARP-1 DBD during 0, 10, 20, and 30 s (Figure 5). The restriction kinetics was stopped by a solution of formamide 90% and EDTA 2 mM. The double-strand DNA and the restricted forms were separated according to their mobility in 15% denaturing gel acrylamide containing 8 M urea and 1 $\times$  TBE and dried on a DE81 filter in a vacuum heater, and the radioactive bands were analyzed using a BioImager (BioRad). A positive control was performed by using the DNA-dependent protein kinase (DNA-PK) at 2.5 nM in the presence of a radioactively labeled DNA substrate with a *Not I* restriction site at 5 nM and digested by the restriction enzyme *Not I*. All the DNA migrations were compared with the migrations of the radiolabeled 60-ds NT alone (60 bp) and digested by *Not I*.

**Steady-State Fluorescence Measurements.** Fluorescence emission spectra were recorded in quartz cells at 20.0 °C ( $\pm 0.5$ ) on a SLM 48 000 spectrofluorimeter. The excitation and emission bandwidths were 2 and 8 nm, respectively. The quantum yield of various complex hPARP-1 DBD/DNA at 295 nm was determined by using L-Trp in water ( $\phi = 0.14$ ) as a reference (20). The binding of hPARP-1 DBD to DNA was monitored using the fluorescence signal of Trp residues present in the protein. Fluorescence titrations were performed by adding increasing amounts of oligonucleotide (Table 1) to a fixed amount of protein in 50 mM Tris-HCl, pH 8, 100 mM NaCl, and 1 mM DTT. The various molar ratios of oligonucleotide to protein were prepared as separate solutions. The excitation wavelength was set at 295 nm.

Steady-state anisotropy measurements were performed with a T-format SLM 8000 spectrofluorimeter at 20 °C. The emitted light was monitored through 350 nm interference filters (Schott). An in-house built device ensured the automatic rotation of the excitation polarizer. Increasing amounts of DNA were added to a fixed amount of hPARP-1 DBD in the same conditions as described above.

**Time-Resolved Fluorescence Measurements.** Time-resolved fluorescence measurements were performed with a time-correlated, single-photon counting technique using the stable excitation pulses provided by a pulse-picked frequency tripled Ti:sapphire laser (Tsunami, Spectra Physics) pumped by a Millennia X laser (Spectra Physics). The temperature was maintained at 20 °C. The excitation pulses were set at 295 nm, with a repetition rate of 4 MHz. The emission was collected through a 4 nm band-pass monochromator (Jobin-Yvon H10) set at 350 nm and a polarizer set at the magic angle (54.7°). The single-photon events were detected with a microchannel plate Hamamatsu R3809U photomultiplier coupled to a Phillips 6954 pulse preamplifier and recorded on a multichannel analyzer (Ortec 7100) calibrated at 25.5 ps/channel. The instrumental response function was recorded with a polished aluminum reflector, and its full-width at half-maximum was 40 ps.

Time-resolved data analysis was performed using the maximum entropy method (MEM) and the Pulse5 software (21). For the analysis of the fluorescence decay, a distribution of 200 equally spaced lifetime values on a logarithmic scale between 0.01 and 10 ns was used. In all cases, the reduced  $\chi^2$  values were close to 1.0, and the weighted residuals as well as the autocorrelation of the residuals were distributed randomly around zero, indicating an optimal fit.

## RESULTS

hPARP-1 is a modular protein, composed of identified domains able to maintain their own well-defined functions when they are isolated from the rest of the protein (11, 22). For instance, previous works showed that the N-terminal 29 kDa Zn $^{2+}$  finger domain of hPARP-1 (Figure 1A) is sufficient to direct specific binding of the whole protein to the target DNA damage (15–17, 23). This fragment of the protein bearing the DNA-binding domain (DBD) was used as model for the analysis of hPARP-1–DNA interactions.

To investigate the DNA features that are relevant for hPARP-1 function, we extended the previous analysis of a 5'-recessed structure (13). We included other 5'-recessed structures differing by the presence or the absence of a different number of telomeric repeats (TTAGGG). Additionally, we analyzed the effect of different DNA features, namely, 3'-recessed structures, double strands, and the presence of a palindromic sequence like a *Not I* restriction site (Table 1 and Figure 1B).

**Binding Parameters of the Interaction between hPARP-1 DBD and Different DNA Substrates.** The hPARP-1 DBD contains four Trp residues whose fluorescence was proved to be sensitive to DNA binding (13). Consequently, the interaction between hPARP-1 DBD and the different DNA substrates (Figure 1B) was investigated by monitoring the tryptophan fluorescence quenching upon addition of oligonucleotide (Figure 2A). Moreover, a remarkable increase in the fluorescence anisotropy was also detected upon DNA

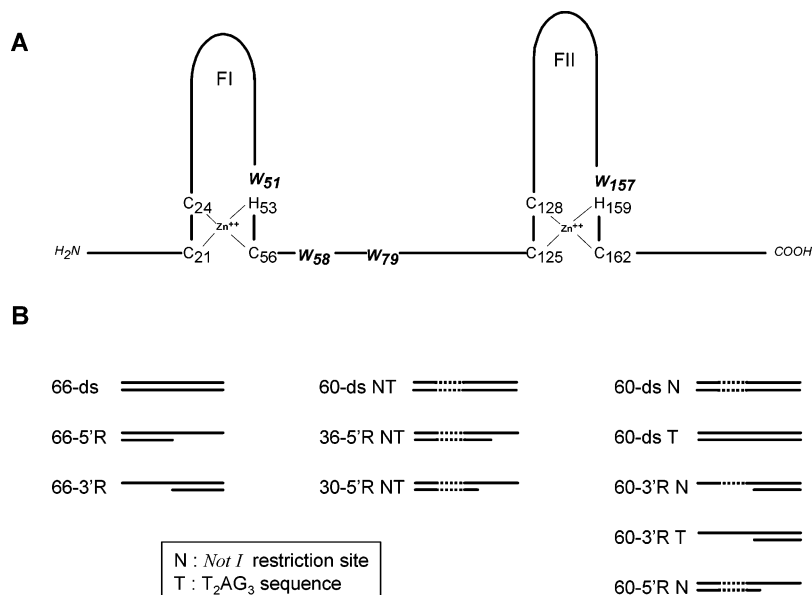
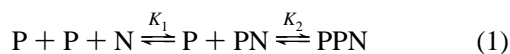


FIGURE 1: (A) Primary structure of the N-terminal DNA binding domain of hPARP-1 (residues 1–234). The DNA-binding domain is drawn to show two zinc-coordinated fingers (FI, FII). The four tryptophans, W51, W58, W79, and W157, are indicated in bold italics. (B) Primary structure of the DNA substrates. Heading numbers in oligonucleotides names refer to the length in bases of the “G” strand, except for 36-5'R NT and 30-5'R NT, which are oligonucleotides differing for the length of the “C” strand, 36 and 30 bases for 36-5'R NT and 30-5'R NT, respectively. The dotted line in the DNA structures indicates the presence of the *Not I* restriction site. Oligonucleotides 60-ds T and 60-3'R T contain various T<sub>2</sub>AG<sub>3</sub> repeats. Oligonucleotides 66-5'R, 36-5'R NT, 30-5'R NT, and 60-5'R N bear a 5'-recessed end. Oligonucleotides 66-3'R, 60-3'R N, and 60-3'R T bear a 3'-recessed end (sequences in Table 1).

binding. Thus, we systematically performed fluorescence anisotropy titrations to corroborate the result obtained by the analysis of the intensity data (Figure 2B). The experiments were performed as described previously (13), to minimize adsorption of the protein onto the walls of the quartz cell and to avoid photobleaching. The binding stoichiometry was determined with the “tangent method”, and the binding data were analyzed using a global strategy to achieve higher accuracy as previously discussed (13).

The binding stoichiometry for the DNA 66-5'R (Figure 2) bearing a 5'-recessed single-stranded break is two hPARP-1 DBD proteins per DNA. The same binding stoichiometry was measured for the oligonucleotide 30-5'R NT. These results are in agreement with our previous finding obtained in the presence of the 36-5'R NT, also bearing a 5'-recessed single-stranded break (13).

The data were analyzed assuming a two-step model with the following reaction scheme:



According to this scheme, the observed fluorescence can be expressed as follows:

$$F = F_P \frac{[P]}{[P]_T} + F_{PN} \frac{K_1 [P] [N]_T}{[P]_T (1 + K_1 [P] + K_1 K_2 [P]^2)} + F_{PPN} \frac{K_1 K_2 [P]^2 [N]_T}{[P]_T (1 + K_1 [P] + K_1 K_2 [P]^2)} \quad (2)$$

where  $K_1$  and  $K_2$  represent the affinity of one protein for the oligonucleotide where none or one protein is already bound, respectively.  $F_P$ ,  $F_{PN}$ , and  $F_{PPN}$  correspond to the fluorescence of the free protein and the complex with one and two

proteins, respectively.  $[P]_T$  and  $[N]_T$  are the total protein and total nucleic acid concentrations, respectively.

Considering that the fluorescence signals of the free and the bound protein are different, the observed fluorescence anisotropy is given by

$$r = \frac{r_P (1 + K_1 [P] + K_1 K_2 [P]^2) + r_{PN} K_1 [N]_T s + r_{PPN} 2s K_1 K_2 [P] [N]_T}{1 + K_1 [P] + K_1 K_2 [P]^2 + [N]_T (s K_1 + 2s K_1 K_2 [P])} \quad (3)$$

where  $r_P$ ,  $r_{PN}$ , and  $r_{PPN}$  represent the anisotropy of the free protein and the complex with one and two proteins, respectively;  $s$  is the ratio between the quantum yield of the bound and the free protein, which is assumed not to change in the presence of an additional bound protein. The free protein concentration  $[P]$  is related to  $[P]_T$ ,  $[N]_T$ ,  $K_1$ , and  $K_2$  by the following cubic equation:

$$[P]^3 + [P]^2 \left( 2[N]_T - [P]_T + \frac{1}{K_2} \right) + [P] \left( \frac{1}{K_1 K_2} + \frac{[N]_T}{K_2} - \frac{[P]_T}{K_2} \right) - \frac{[P]_T}{K_1 K_2} = 0 \quad (4)$$

By applying a global analysis to anisotropy and intensity data together, we obtained  $K_1 = 1.68 \times 10^7 \text{ M}^{-1}$  and  $K_2 = 1.35 \times 10^8 \text{ M}^{-1}$ , in the case of the oligonucleotide 66-5'R and  $K_1 = 1.0 \times 10^4 \text{ M}^{-1}$  and  $K_2 = 3.56 \times 10^9 \text{ M}^{-1}$  in the case of oligonucleotide 30-5'R NT. These results show that the second protein binds with higher affinity than the first protein, indicating a cooperative binding between the two proteins (24). The “all-or-none” mechanism that was used to analyze the interaction between hPARP-1 DBD and 36-5'R NT where two hPARP-1 DBD proteins bind with infinite cooperativity (13) could not be applied to analyze the

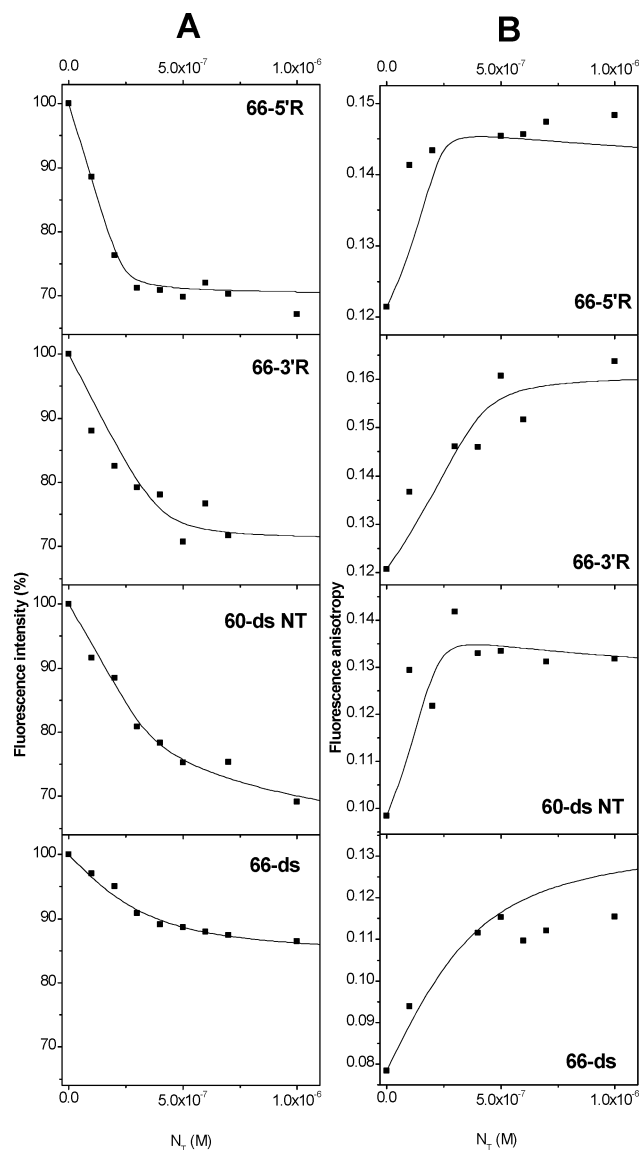


FIGURE 2: Titration curves for binding of hPARP-1 DBD to the 66-5'R, the 66-3'R, the 60-ds NT, and the 66-ds oligonucleotides. hPARP-1 DBD concentration was 0.5, 0.4, 0.45, and 0.3  $\mu\text{M}$ , respectively. (A) Fluorescence intensity data. The solid lines correspond to the fits to the experimental data. Eqs 2 and 4 were used to generate the theoretical curve in case of 66-5'R and 60-ds NT, while eqs 6 and 8 were used to generate the theoretical curve in case of 66-3'R and 66-ds, as explained in the text. (B) Fluorescence anisotropy data. Solid lines correspond to the fits to the experimental data. Eqs 3 and 4 were used to generate the theoretical curve in case of 66-5'R and 60-ds NT, while eqs 7 and 8 were used to generate the theoretical curve in case of 66-3'R and 66-ds, as explained in the text.

interaction of hPARP-1 DBD with 66-5'R and 30-5'R NT, because  $K_2$  is not sufficiently higher than  $K_1$ . Nevertheless, 66-5'R and 30-5'R NT bind two hPARP-1 DBD proteins with a positive cooperativity, indicating that a 5'-recessed structure recruits two hPARP-1 proteins.  $K_1$  and  $K_2$  can be related to the affinity constant determined from the infinite cooperative model,  $K_\infty$ , by the relation  $K_\infty = K_1K_2$ . Interpreted in this way, the stability constants of the two-protein complex of 66-5'R and of 30-5'R NT are  $K_1K_2 = 2.27 \times 10^{15} \text{ M}^{-2}$  and  $K_1K_2 = 3.56 \times 10^{13} \text{ M}^{-2}$ , respectively. Thus, both values are in line with  $K_\infty = 1.4 \times 10^{14} \text{ M}^{-2}$  found for the two-protein complex with 36-5'R NT (13). This result denotes that a 5'-recessed DNA structure represents a high affinity

binding site for two hPARP-1 DBD proteins, independent of the sequence.

The hPARP-1 DBD complexes with the oligonucleotides 66-ds and 66-3'R show a stoichiometry of 1:1 (Figure 2). The oligonucleotide 66-ds is a double-strand DNA, while 66-3'R is a DNA with the same "G" strand and bearing a 3'-recessed single-strand break. The data were thus analyzed assuming the following one-step reaction scheme:



implying the following equations to fit the fluorescence signal,

$$F = \frac{F_P(1 + K[P]) + F_{PN}K[N]_T}{1 + K[P] + K[N]_T} \quad (6)$$

and the anisotropy signal,

$$r = \frac{r_P(1 + K[P]) - r_{PN}K[N]_T s}{1 + K[P] + sK[N]_T} \quad (7)$$

where  $F_P$  and  $r_P$  are the fluorescence intensity and anisotropy signals of the free protein and  $F_{PN}$  and  $r_{PN}$  are the fluorescence intensity and anisotropy signals of the complex;  $s$  represent the ratio between the quantum yield of the bound and the free protein.

The free protein concentration is related to the total protein  $[P]_T$  and total nucleic acid  $[N]_T$  concentrations by the following equation:

$$[P]^2 + [P]([N]_T - [P]_T + \frac{1}{K}) - \frac{[P]_T}{K} = 0 \quad (8)$$

The equilibrium association constants,  $K$ , are  $8 \times 10^6 \text{ M}^{-1}$  and  $7 \times 10^7 \text{ M}^{-1}$  in case of the double-strand 66-ds and the 3'-recessed single-strand break DNA 66-3'R, respectively.

In contrast, in the case of the double-strand 60-ds NT, the binding mode is less clear, because the stoichiometry is not well-defined and found to be between one and two proteins per DNA. The analysis of the binding data with the two-step model provides similar values for  $K_1$  and  $K_2$  of about  $4 \times 10^7 \text{ M}^{-1}$ , indicating that the first and the second protein bind to 60-ds NT with equal affinity. When the binding constants  $K_1$  and  $K_2$  are equal, the two-protein complex will be populated only if the DNA concentration is lower than the protein concentration. On the contrary, when DNA is in large excess, only one protein will bind per DNA molecule. The change in the proportion between the populations of the two-protein complex and the one-protein complex during the titration can explain the difficulty in determining a clear stoichiometry.

To get additional information on the involvement of Trp residues in the interaction between hPARP-1 DBD and DNA, a time-resolved fluorescence investigation was performed. The fluorescence decay parameters of the free protein and of the protein in the complex with the oligonucleotides 30-5'R NT, 66-5'R, 60-ds NT, 66-ds, and 66-3'R are reported in Table 2. In all cases, the lifetime distribution is trimodal. In the free protein, the time-resolved profile is characterized by a mean lifetime of 2.75 ns and is dominated by the longest lifetime of 4.98 ns which contributes about 75% to the total

Table 2: Fluorescence Decay Parameters of hPARP-1 DBD in the Free Form and in the Complexes with Various DNA Substrates

	$\tau_i$ (ns) <sup>a</sup>	$\alpha_i$ <sup>a</sup>	$f_i$ <sup>a</sup>	$\langle\tau\rangle$ (ns) <sup>a</sup>
hPARP-1 DBD <sup>b</sup>	4.98 ± 0.03	0.41 ± 0.02	0.74 ± 0.03	2.75 ± 0.02
free	1.59 ± 0.07	0.40 ± 0.01	0.23 ± 0.02	
	0.34 ± 0.01	0.19 ± 0.01	0.02 ± 0.01	
+ 30-5'R NT	4.07 ± 0.02	0.11 ± 0.03	0.49 ± 0.01	0.95 ± 0.01
	1.30 ± 0.01	0.33 ± 0.01	0.45 ± 0.03	
	0.10 ± 0.04	0.55 ± 0.02	0.06 ± 0.01	
+ 66-5'R	3.75 ± 0.01	0.23 ± 0.03	0.55 ± 0.01	1.56 ± 0.03
	1.19 ± 0.01	0.56 ± 0.02	0.43 ± 0.04	
	0.17 ± 0.02	0.21 ± 0.02	0.02 ± 0.01	
+ 60-ds NT	4.03 ± 0.05	0.15 ± 0.02	0.49 ± 0.03	1.24 ± 0.01
	1.30 ± 0.01	0.45 ± 0.02	0.47 ± 0.01	
	0.12 ± 0.01	0.40 ± 0.01	0.04 ± 0.03	
+ 66-ds	4.08 ± 0.01	0.23 ± 0.04	0.57 ± 0.02	1.65 ± 0.01
	1.22 ± 0.01	0.55 ± 0.01	0.41 ± 0.02	
	0.18 ± 0.02	0.22 ± 0.02	0.02 ± 0.01	
+ 66-3'R	4.17 ± 0.03	0.20 ± 0.02	0.51 ± 0.01	1.59 ± 0.02
	1.30 ± 0.01	0.57 ± 0.02	0.47 ± 0.01	
	0.15 ± 0.01	0.23 ± 0.04	0.02 ± 0.02	

<sup>a</sup> The fluorescence lifetimes ( $\tau_i$ ), the relative amplitudes ( $\alpha_i$ ), the fractional intensities ( $f_i$ ), and the mean lifetimes ( $\langle\tau\rangle$ ) are expressed as means  $\pm$  the standard error of the mean for three experiments. The width of the distribution associated with each lifetime was found to be narrow under each condition, being less than 20% of the value of the lifetime. The mean lifetime was calculated with  $\langle\tau\rangle = \sum\alpha_i\tau_i$ . Excitation and emission wavelengths are 295 and 350 nm, respectively. hPARP-1 DBD and DNA concentrations are 1 and 1.5  $\mu$ M, respectively. <sup>b</sup> Values from Pion et al. (13).

fluorescence. When the protein is bound to 66-ds or 66-3'R, the lifetime distribution remains trimodal. However, in both complexes, the fluorescence decay is characterized by a mean lifetime of about 1.6 ns which is 40% lower than the lifetime of the free protein. Moreover, the profile of the lifetime in both complexes is identical. The two major lifetimes are about 4.1 and 1.3 ns with associated amplitude of about 0.2 and 0.55, respectively, and a minor lifetime of about 0.2 ns. This high similarity of the time-resolved fluorescence parameters indicates that the same classes of Trp conformers are selected in both complexes, suggesting that hPARP-1 DBD binds to 66-ds and 66-3'R in a similar way.

The comparison of the fluorescence decay parameters of the protein in the complex with the oligonucleotides 66-ds, 66-5'R, 60-ds NT, and 30-5'R NT provide additional information (Table 2). In all the complexes, the lifetime distribution is trimodal as in the free protein, but the mean lifetime is lower, following the order 66-ds > 66-5'R > 60-ds NT > 30-5'R NT. All the DNA-protein complexes display very similar sets of three lifetimes, where each lifetime was shortened by about 20% as compared to the corresponding lifetime in the free protein. Thus, to explain the differences in the mean lifetimes among the complexes, it is necessary to analyze the amplitude distribution. When hPARP-1 DBD binds to one of these DNA substrates, the major effect is the decrease of the amplitude of the longest lifetime to the benefit of the others. However, when hPARP-1 DBD is bound to DNA lacking the *Not I* site (66-5'R and 66-ds), the amplitude decrease of the long-lived component is compensated by the amplitude increase of the intermediate component. Differently, when hPARP-1 DBD is bound to the DNA bearing the *Not I* restriction site (30-5'R NT and 60-ds NT), the amplitude of the long-lived component decreases to the benefit of the shortest component. This result indicates that the binding of DNA containing a *Not I*

restriction site favors the conformers where the Trp is more quenched, indicating the hPARP-1 DBD binding mode to DNA with and without a *Not I* restriction site is different.

**DNA Binding Detected by Footprinting Experiments.** The hPARP-1 DBD purified as previously described (16) was incubated with various labeled DNA substrates and processed for footprinting experiments (Figure 3). In the case of 30-5'R NT, which bears a single-stranded, 5'-recessed break accompanied by a single telomeric repeat, a specific binding of the hPARP-1 DBD occurs at the junction between the double-stranded and the single-stranded portion; 21 nucleotides are protected (Figure 3B, lane i). A protection was previously found also when the size of the "C" strand was prolonged by one telomeric repeat (probe 36-5'R-NT), even if in that case the footprint was shifted by 2 nucleotides and a shorter region (11 nucleotides) was protected (13). Nevertheless, protection appears independent of the presence of telomeric repeats. In fact, 11 nucleotides are protected also in the probe 66-5'R (Figure 3B, lane b), where telomeric repeats are absent. Oligonucleotides 30-5'R NT and 36-5'R NT have in common the presence of a *Not I* restriction site, differing by its proximity to the 5'-end of the junction. The different proximity between *Not I* restriction site and the 5'-end of the junction may be responsible for the difference in the footprint in these two DNA substrates, indicating that the *Not I* restriction site may influence hPARP-1 binding. In contrast, no protection was observed using the double-stranded probes 60-ds NT (Figure 3B, lane h) or an oligonucleotide bearing a 3'-recessed single-stranded break, indicating that hPARP-1 binds these oligonucleotides less strongly.

**The Effect of the DNA Structure on hPARP-1 Activity.** To evaluate the effect of the DNA structure on hPARP-1 activity, we measured the extent of poly(ADP-ribose) formation induced by the interaction of hPARP-1 with several DNA differing by their structure or their sequence (Figure 4). A DNase I-activated DNA, which is known to induce hPARP-1 activity, was used as a reference, and the hPARP-1 activity induced by this DNA was set to 100%. Accordingly, the values of hPARP-1 activity caused by each of the DNA fragments are expressed relative to this reference. Clearly, the in vitro poly(ADP-ribose) synthesis stimulated by DNA strand breaks was affected by the DNA structure. The highest hPARP-1 activity in the range of 130–150% was observed for oligonucleotides bearing a 5'-recessed end, independently of the sequence (probes 66-5'R, 30-5'R NT, 36-5'R NT, and 60-5'R N). In contrast, the lowest activity of about 40–50% was found in the presence of 3'-recessed DNA ends (66-3'R, 60-3'R N, and 60-3'R T). These results show that hPARP-1 can discriminate between 5'- and 3'-recessed ends.

As previously reported, hPARP-1 is activated in the presence of single-strand breaks on DNA (17). Therefore, double-stranded DNA is expected not to induce enzyme activity. Accordingly, a low percentage of activity was found in the presence of the oligonucleotide 66-ds (Figure 4). In contrast, a surprisingly high activity of 140% was detected in the presence of the double-strand 60-ds NT. The oligonucleotide 60-ds NT possesses two particular sequence features: a *Not I* restriction site and TTAGGG telomeric repeats. Both sequence features could be potential recognition sites for hPARP-1. To clarify which feature is preferentially recognized by hPARP-1, we tested the ability of one double-

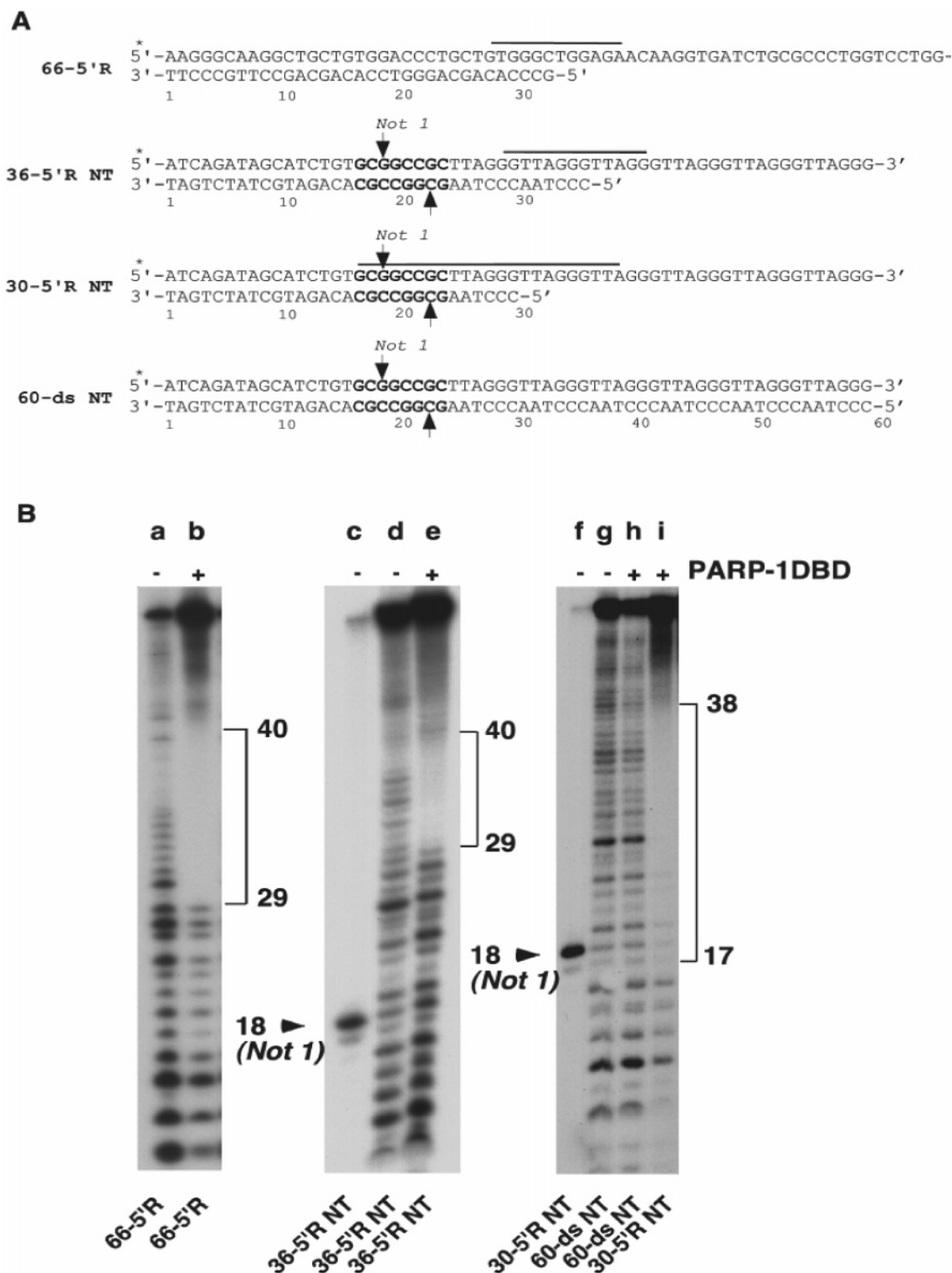


FIGURE 3: (A) Sequences of the oligonucleotides used for footprinting experiments. The black lines indicate the protected region, and the bold capital letters represent the *Not I* restriction sites. (B) DNase I footprint of hPARP-1 DBD on the DNA described in panel A. The experiments were performed according to the method in ref 17. The signs (+) and (-) indicate the presence and absence of hPARP-1 DBD, respectively. The arrowheads indicate *Not I* digestion of 36-5'R NT and 30-5' R NT oligonucleotides (lanes c and f, respectively) confirming the annealing.

stranded DNA bearing only the TTAGGG repeats (probe 60-ds T) and of one containing only the *Not I* restriction site (probe 60-ds N) to induce hPARP-1 activity. The considerably higher activity of probe 60-ds N compared to probe 60-ds T shows that the presence of a restriction site such as a *Not I* site strongly enhances hPARP-1 activity. To examine if the increase of hPARP-1 activity in the presence

of double-strand DNA bearing a *Not I* restriction site can be directly related to the specific recognition for such a sequence, we tested the ability of hPARP-1 DBD to protect the oligonucleotide 60-ds NT against the action of the restriction enzyme *Not I* (Figure 5). The radiolabeled double-strand DNA was incubated with the restriction enzyme *Not I* in the presence or in the absence of the hPARP-1 DBD.



case, the estimation of the bound species is influenced by the degree of reactivity.

The impact of the type of DNA-break end on hPARP-1 behavior was directly compared using 66-3'R and 66-5'R. These two DNA substrates differ only in the break end, 3' for 66-3'R and 5' for 66-5'R. A clear difference between a 5'-recessed and a 3'-recessed DNA structure, both in the binding mode and in the hPARP-1 activation, is observed. In fact, in contrast to the protein complex with a 5'-recessed structure which displays a stoichiometry of two proteins per one DNA molecule, hPARP-1 DBD binds 3'-recessed structures with a 1:1 stoichiometry. The stability constant for a 3'-recessed structure is about  $10^8 \text{ M}^{-1}$ , which is very similar to the mean affinity of one protein to the 5'-recessed structures ( $\sqrt{K_1 K_2}$  in the reaction Scheme 1). Moreover, the hPARP-1 activity induced by a 3'-recessed structure is the lowest among the tested DNA substrates, while the activity induced by a 5'-recessed structure is the highest.

An important feature that emerges from our study is the link existing between hPARP-1 dimerization and its activation. In fact, the 5'-recessed structure, on one hand, provokes the highest hPARP-1 activation and, on the other hand, it implies tight protein complexes whose stability is enhanced by the positive cooperativity. In contrast, a 3' junction does not appear suitable for hPARP-1 binding as indicated by the absence of footprint. These findings not only strengthen the hypothesis that dimerization has an impact on hPARP-1 function by enhancing its activity but also show that hPARP-1 specifically recognizes 5'-recessed structures as an important factor for its activation. In addition, we can support the hypothesis that even in a single-stranded DNA nick, hPARP-1 recognizes mainly the 5'-end of the nick, leaving the 3'-end free of access to DNA 3'-end processing enzymes that contribute to base excision repair (6). Moreover, PARP-1 can encounter 5'-recessed DNA structures, not only during DNA damage induced by alkylating agents, but also during an active transcription process when topoisomerase I stalls and transient 5' DNA ends are produced. In fact, it has been reported that PARP-1 is strongly stimulated by these 5'-recessed DNA ends (27).

*hPARP-1 Activity in the Presence of Double Strand End.* hPARP-1 DBD binds the double-strand substrate 66-ds with the stoichiometry 1:1 as in the complex with 66-3'R. Moreover, hPARP-1 DBD displays very similar time-resolved fluorescence parameters in the presence of both DNA substrates (Table 2), and in both cases, no protected regions are revealed by footprinting experiments. Thus, although the binding affinity of hPARP-1 DBD for 66-3'R bearing a 3'-recessed structure is about 9-fold higher than for the double-strand 66-ds, the protein is expected to bind the two types of oligonucleotides in a similar way. A possible binding site for hPARP-1 DBD to these DNA substrates is the double-strand end which is common to both oligonucleotides. The conclusion that hPARP-1 binds at the end of the double strand is in line with the absence of a protected region on both 66-ds and 66-3'R in the footprinting experiments. As far as the double-strand DNA is concerned, a similar behavior was found also for the human replication protein A (RPA). Indeed, an atomic force microscopy study revealed that RPA binds to undamaged double-strand DNA at its

terminus (28). Similarly, the zinc finger domain of Ligase III $\alpha$  was found to bind to double-stranded ends in DNA (29).

The hPARP-1 activity detected in the presence of double-strand and 3'-recessed end DNA fragments is similar, and even if low, it is not negligible. This phenomenon is surprising since hPARP-1 is expected to function as a catalytic dimer (13, 14, 30) and no evidence of protein dimerization was found in the presence of these DNA substrates for which the binding stoichiometry is only one protein per DNA molecule. Therefore, in agreement with the analysis of the binding data and the footprint experiments which suggest that hPARP-1 DBD binds these DNA substrates at their double-strand end, we propose that the detectable hPARP-1 activity is due to a transient contact of two hPARP-1 molecules, each one bound to the end of a different DNA fragment. This hypothesis is in line with the work of Calsou and co-workers, which showed that hPARP-1 is able to bring together two oligonucleotides (31).

*The Structural Motif Connected to a Restriction Site like a Not I Site May Be a Recognition Site for hPARP-1.* The results of our study show that a restriction site such as a *Not I* site has an effect on hPARP-1 functions. In fact, the presence of a *Not I* restriction site in the double-strand 60-ds NT markedly increases the hPARP-1 activity as compared to the effect of a double strand lacking the *Not I* restriction site. Moreover, in 60-ds NT, the stoichiometry was about 2:1 evoking the possibility for protein dimerization.

The hypothesis that the structural motif connected to a restriction site such as a *Not I* site is a recognition site for hPARP-1 is corroborated by the time-resolved fluorescence data. The comparison of the decay profile of the hPARP-1 DBD complex with DNA bearing the *Not I* restriction site (30-5'R NT and 60-ds NT) or not bearing it (66-5'R and 66-ds) indicates that the binding of DNA containing a *Not I* restriction site favors the conformers where the Trp is more quenched (Table 2), pointing to a specific involvement of the Trp residues in binding. To further understand the molecular basis of the recognition process, the determination of the 3D structure of hPARP-1 DBD in complex with a DNA target will be of great help.

The *Not I* digestion experiment indicates that the *Not I* restriction site represents a recognition site for hPARP-1. Indeed, when 60-ds NT is in the presence of hPARP-1 DBD, the digestion by *Not I* becomes impossible, indicating that hPARP-1 DBD protects this DNA region against the digestion by binding to it. This protection is not found when the same DNA is in the presence of DNA-PK. DNA-PK is known to bind to DNA termini (25); therefore, the *Not I* restriction site remains free and thus accessible to a more specific enzyme like hPARP-1. The same conclusion was reached by using oligonucleotides with each strand containing a 5'-biotinylated end, similarly to ref 32. In the double-strand oligonucleotide containing the *Not I* binding site (same nucleotide sequence as 60-ds NT), the presence of the biotine at the double-strand end did not modify both the binding and the activity parameters. In contrast, in the double-strand oligonucleotide not containing the *Not I* binding site (same nucleotide sequence as 66-ds), where the protein is supposed to bind at the double-strand end, binding was perturbed. These results further support the conclusion that the *Not I* binding site is recognized by hPARP-1.

DNA	Bound proteins	PARP activity	Binding model
66-ds 	1	low	
66-5'R 	2	high	
66-3'R 	1	low	
60-ds NT 	2	high	

FIGURE 6: Binding modes of hPARP-1 with the various DNA substrates. The structure of the different DNA substrates is represented in the first column, in order from above: double strand, 5'-recessed end, 3'-recessed end, structure presenting a *Not I* restriction site. In the second column, the number of the proteins bound to the corresponding DNA substrate is listed. In the third column, the amount of the corresponding enzymatic activity of hPARP-1 is reported. The proposed models of binding between hPARP-1 and the various DNA substrates are represented in the fourth column. A high activity of poly(ADP-ribosylation) is always related to a stoichiometry of two proteins per DNA. In the protein dimer, one protein is expected to act as donor (d) of poly(ADP-ribose) and the other as an acceptor (a).

A *Not I* site, as most of the restriction sites, is constituted of a palindromic sequence, which is known to favor hairpin formation (33). In particular, tracts of GC base pair have an unusually rapid base pair dynamics implying a transient spontaneous opening (34). The specificity of hPARP-1 for the hairpin resulting from the structuration of the palindromic sequence is in agreement with previous observations about the ability of hPARP-1 to bind cruciforms DNA (11, 35–38). It was also shown that in the absence of strand breaks hPARP-1 binds to various structural discontinuities such as three- or four-way junctions, bent DNA, base-unpaired region, and hairpin in DNA heteroduplex (39). Similarly, PARP-like zinc fingers of a repair protein from *Arabidopsis thaliana*, AtZDP, can protect bulge sites on DNA (40), confirming that a structural motif connected to this feature plays a role in stimulating hPARP-1. In addition, previous studies of PARP-1 (37, 41, 42) and AtZDP (43) using electron microscopy and atomic force microscopy have shown that DNA structures that are able to bind to PARP-like zinc fingers adopt sharply kinked V-shaped structures when bound. In our case, the presence of a sharp angle implying a V-shaped structure could be the common feature between the hairpin structure induced by a *Not I* restriction site and the 5'-recessed structure whose flexibility has been shown to allow DNA bending (42, 44). These kinked structures could allow an optimal fitting of the PARP-1 proteins into the DNA backbone entailing its strong activation. For example, the DNA torsion could facilitate the recruitment of others PARP-1 partners implicated in the protection and the repair of DNA. Similar kinked structures were also described for others DNA binding proteins implicated in DNA repair or DNA recombination like HU protein or T7 endonuclease I protein (45, 46).

The finding that a site like *Not I* appears as a coactivator of PARP-1 strengthens the spreading idea that PARP-1 has also some function in the undamaged cells. A number of

studies have examined PARP-1 as a regulator of chromatin structure and transcription. These data have been used to support a model whereby PARP-1 promotes the decondensation of chromatin through (ADP-ribosylation) of H1 and core histones as well as the generation of polyanionic, histone-binding poly(ADP-ribose) (36, 47–50). However, the molecular determinants for PARP-1 recruitment to the specific chromatin site in normally functioning cells (in the absence of genotoxic stress) are still unclear. Binding to non-B DNA structures, such as hairpin, cruciforms, and unwound regions that can form in the transcriptional regulatory elements, many of which contains palindromic sequence, could represent a way for PARP-1 recruitment to specific chromatin sites.

## CONCLUSION

The automodification of the catalytic domain alone proceeds via formation of a homodimer also in absence of DNA (51). Nevertheless, in the presence of DNA, the full length hPARP-1 is more efficiently poly(ADP)ribosylated than the catalytic domain alone, suggesting that the binding promoted by the hPARP-1 DBD prompted the protein activity. There is clear evidence that PARP-like fingers can communicate their DNA-binding status to the associated catalytic domains. In PARPs, the enzymatic activity is strongly activated upon DNA-break recognition (52).

In this context, our work underlines that dimerization is a prerequisite for hPARP-1 activation. Moreover, the specificity of hPARP-1 for 5'-end of the junction against a 3'-end is clearly evinced, and it could be considered as a rationale for the way in which hPARP-1 operates in damaged cells. Our study illustrates that the 5' junction recruits two proteins to form a catalytic dimer responsible of the high activity detected for this DNA substrate. In contrast, a 3' junction does not appear suitable for hPARP-1 binding. Indeed, hPARP-1 DBD binds a 3'-recessed structure at the double-strand end with a stoichiometry of 1:1. Therefore, the residual hPARP-1 activity that is detected should be attributed to the transient contact of two hPARP-1 proteins, each one bound at the double-strand end of different DNA fragments. A similar mechanism can explain the binding and activity data in the presence of an undamaged double-strand DNA fragment. Binding of DNA by PARP-like fingers is essentially independent of the DNA sequence (17); instead, what is relevant for PARP functions is the recognition of overall features, such as, for example, kinked structures. In fact, since the DNA damage can be a random event, proteins that are implied in repairing DNA damages, such as hPARP-1, should be able to function independently of the sequence context.

In this paper, we show also the impact of a restriction site like a *Not I* site on hPARP-1 activation. The presence of a *Not I* restriction site in a double strand increases significantly the hPARP-1 activity. The important enhancement in protein activity is attributed to the possibility of the formation of a hairpin structure in the DNA. This finding brings additional evidence that hPARP-1 may have a role in the modulation of chromatin structure in the absence of breaks, in agreement with very recent studies (53, 54). hPARP-1 activation upon binding to non-B DNA structures may lead to a modification of histone and nonhistone proteins where such structures are

formed. PARP-1 self-inactivation induced by automodification and subsequent dissociation from DNA would ensure a transient character of chromatin poly(ADP-ribosylation). Our conclusions on the binding modes of hPARP-1 are illustrated in Figure 6.

## ACKNOWLEDGMENT

We are grateful to Dr. Josiane Ménissier-de Murcia for the footprinting experiments, to Etienne Piémont, Dr. Katia Zanier, Dr. Serena Bernacchi, and Aline Huber for technical assistance and to Dr. David Llères for careful reading of the manuscript.

## REFERENCES

- Ame, J. C., Spenlehauer, C., and de Murcia, G. (2004) The PARP superfamily, *BioEssays* 26, 882–893.
- Caldecott, K. W. (2003) Cell signaling. The BRCT domain: signaling with friends?, *Science* 302, 579–580.
- Trucco, C., Oliver, F. J., de Murcia, G., and Menissier-de Murcia, J. (1998) DNA repair defect in poly(ADP-ribose) polymerase-deficient cell lines, *Nucleic Acids Res.* 26, 2644–2649.
- Panzeter, P. L., Zweifel, B., Malanga, M., Waser, S. H., Richard, M., and Althaus, F. R. (1993) Targeting of histone tails by poly(ADP-ribose), *J. Biol. Chem.* 268, 17662–17664.
- Masson, M., Niedergang, C., Schreiber, V., Muller, S., Menissier-de Murcia, J., and de Murcia, G. (1998) XRCC1 is specifically associated with poly(ADP-ribose) polymerase and negatively regulates its activity following DNA damage, *Mol. Cell. Biol.* 18, 3563–3571.
- Okano, S., Lan, L., Caldecott, K. W., Mori, T., and Yasui, A. (2003) Spatial and temporal cellular responses to single-strand breaks in human cells, *Mol. Cell. Biol.* 23, 3974–3981.
- Lan, L., Nakajima, S., Oohata, Y., Takao, M., Okano, S., Masutani, M., Wilson, S. H., and Yasui, A. (2004) In situ analysis of repair processes for oxidative DNA damage in mammalian cells, *Proc. Natl. Acad. Sci. U.S.A.* 101, 13738–13743.
- Benjamin, R. C., and Gill, D. M. (1980) Poly(ADP-ribose) synthesis in vitro programmed by damaged DNA. A comparison of DNA molecules containing different types of strand breaks, *J. Biol. Chem.* 255, 10502–10508.
- Hengartner, C., Lagueux, J., and Poirier, G. G. (1991) Analysis of the activation of poly(ADP-ribose) polymerase by various types of DNA, *Biochem. Cell Biol.* 69, 577–580.
- Dantzer, F., Schreiber, V., Niedergang, C., Trucco, C., Flatter, E., De La Rubia, G., Oliver, J., Rolli, V., Menissier-de Murcia, J., and de Murcia, G. (1999) Involvement of poly(ADP-ribose) polymerase in base excision repair, *Biochimie* 81, 69–75.
- de Murcia, G., and Shall, S. (2000) *From DNA Damage and Stress Signalling to Cell Death. Poly ADP-Ribosylation Reactions*, Oxford University Press, Oxford, U.K.
- D’Silva, I., Pelletier, J. D., Lagueux, J., D’Amours, D., Chaudhry, M. A., Weinfeld, M., Lees-Miller, S. P., and Poirier, G. G. (1999) Relative affinities of poly(ADP-ribose) polymerase and DNA-dependent protein kinase for DNA strand interruptions, *Biochim. Biophys. Acta* 1430, 119–126.
- Pion, E., Bombarda, E., Stiegler, P., Ullmann, G. M., Mely, Y., de Murcia, G., and Gerard, D. (2003) Poly(ADP-ribose) polymerase-1 dimerizes at a 5′ recessed DNA end in vitro: a fluorescence study, *Biochemistry* 42, 12409–12417.
- Mendoza-Alvarez, H., and Alvarez-Gonzalez, R. (1993) Poly(ADP-ribose) polymerase is a catalytic dimer and the automodification reaction is intermolecular, *J. Biol. Chem.* 268, 22575–22580.
- Gradwohl, G., Menissier de Murcia, J., Molinete, M., Simonin, F., and de Murcia, G. (1989) Expression of functional zinc finger domain of human poly(ADP-ribose) polymerase in *E. coli*, *Nucleic Acids Res.* 17, 7112.
- Molinete, M., Vermeulen, W., Burkle, A., Menissier-de Murcia, J., Kupper, J. H., Hoeijmakers, J. H., and de Murcia, G. (1993) Overproduction of the poly(ADP-ribose) polymerase DNA-binding domain blocks alkylation-induced DNA repair synthesis in mammalian cells, *EMBO J.* 12, 2109–2117.
- Menissier-de Murcia, J., Molinete, M., Gradwohl, G., Simonin, F., and de Murcia, G. (1989) Zinc-binding domain of poly(ADP-ribose) polymerase participates in the recognition of single strand breaks on DNA, *J. Mol. Biol.* 210, 229–233.
- Simonin, F., Hofferer, L., Panzeter, P. L., Muller, S., de Murcia, G., and Althaus, F. R. (1993) The carboxyl-terminal domain of human poly(ADP-ribose) polymerase. Overproduction in *Escherichia coli*, large scale purification, and characterization, *J. Biol. Chem.* 268, 13454–13461.
- Niedergang, C., Okazaki, H., and Mandel, P. (1979) Properties of purified calf thymus poly(adenosine diphosphate ribose) polymerase. Comparison of the DNA-independent and the DNA-dependent enzyme, *Eur. J. Biochem.* 102, 43–57.
- Eisinger, J., and Navon, G. (1969) Fluorescence quenching and isotope effect of tryptophan, *J. Chem. Phys.* 50, 2069–2077.
- Livesey, A. K., and Brochon, J. C. (1987) Analyzing the distribution of decay constants in pulse-fluorimetry using the maximum entropy method, *Biophys. J.* 52, 693–706.
- Mazen, A., Menissier-de Murcia, J., Molinete, M., Simonin, F., Gradwohl, G., Poirier, G., and de Murcia, G. (1989) Poly(ADP-ribose) polymerase: a novel finger protein, *Nucleic Acids Res.* 17, 4689–4698.
- Gradwohl, G., Menissier de Murcia, J. M., Molinete, M., Simonin, F., Koken, M., Hoeijmakers, J. H., and de Murcia, G. (1990) The second zinc-finger domain of poly(ADP-ribose) polymerase determines specificity for single-stranded breaks in DNA, *Proc. Natl. Acad. Sci. U.S.A.* 87, 2990–2994.
- Onufriev, A., and Ullmann, G. M. (2004) Decomposing complex cooperative ligand binding into simple components: connections between microscopic and macroscopic models, *J. Phys. Chem. B* 108, 11157–11169.
- Durocher, D., and Jackson, S. P. (2001) DNA-PK, ATM and ATR as sensors of DNA damage: variations on a theme?, *Curr. Opin. Cell Biol.* 13, 225–231.
- D’Amours, D., Sallmann, F. R., Dixit, V. M., and Poirier, G. G. (2001) Gain-of-function of poly(ADP-ribose) polymerase-1 upon cleavage by apoptotic proteases: implications for apoptosis, *J. Cell Sci.* 114, 3771–3778.
- Malanga, M., and Althaus, F. R. (2004) Poly(ADP-ribose) reactivates stalled DNA topoisomerase I and induces DNA strand break resealing, *J. Biol. Chem.* 279, 5244–5248.
- Lysetska, M., Knoll, A., Boehringer, D., Hey, T., Krauss, G., and Krausch, G. (2002) UV light-damaged DNA and its interaction with human replication protein A: an atomic force microscopy study, *Nucleic Acids Res.* 30, 2686–2691.
- Kulczyk, A. W., Yang, J. C., and Neuhaus, D. (2004) Solution structure and DNA binding of the zinc-finger domain from DNA ligase IIIalpha, *J. Mol. Biol.* 341, 723–738.
- Bauer, P. I., Buki, K. G., Hakam, A., and Kun, E. (1990) Macromolecular association of ADP-ribosyltransferase and its correlation with enzymic activity, *Biochem. J.* 270, 17–26.
- Audebert, M., Salles, B., and Calsou, P. (2004) Involvement of poly(ADP-ribose) polymerase-1 and XRCC1/DNA ligase III in an alternative route for DNA double-strand breaks rejoining, *J. Biol. Chem.* 279, 55117–55126.
- Parsons, J. L., Dianova, I. I., Allinson, S. L., and Dianov, G. L. (2005) Poly(ADP-ribose) polymerase-1 protects excessive DNA strand breaks from deterioration during repair in human cell extracts, *FEBS J.* 272, 2012–2021.
- Sambrook, J., Fritsch, E. F., and Maniatis, T. (1989) *Molecular Cloning*, Vol. 2, Cold Spring Harbor Laboratory Press, Cold Spring Harbor, NY.
- Dornberger, U., Leijon, M., and Fritzsche, H. (1999) High base pair opening rates in tracts of GC base pairs, *J. Biol. Chem.* 274, 6957–6962.
- Szabo, C. (2002) PARP as a drug target for the therapy of diabetic cardiovascular dysfunction, *Drug News Perspect.* 15, 197–205.
- D’Amours, D., Desnoyers, S., D’Silva, I., and Poirier, G. G. (1999) Poly(ADP-ribose) polymerase-1 and XRCC1/DNA ligase III in the regulation of nuclear functions, *Biochem. J.* 342 (Pt 2), 249–268.
- Gradwohl, G., Mazen, A., and de Murcia, G. (1987) Poly(ADP-ribose) polymerase forms loops with DNA, *Biochem. Biophys. Res. Commun.* 148, 913–919.
- Sastry, S. S., and Kun, E. (1990) The interaction of adenosine diphosphoribosyl transferase (ADPRT) with a cruciform DNA, *Biochem. Biophys. Res. Commun.* 167, 842–847.
- Soldatenkov, V. A., and Potaman, V. N. (2004) DNA-binding properties of poly(ADP-ribose) polymerase: a target for anticancer therapy, *Curr. Drug Targets* 5, 357–365.
- Petrucchio, S. (2003) Sensing DNA damage by PARP-like fingers, *Nucleic Acids Res.* 31, 6689–6699.

41. Smulson, M. E., Pang, D., Jung, M., Dimtchev, A., Chasovskikh, S., Spoonde, A., Simbulan-Rosenthal, C., Rosenthal, D., Yakovlev, A., and Dritschilo, A. (1998) Irreversible binding of poly(ADP-ribose) polymerase cleavage product to DNA ends revealed by atomic force microscopy: possible role in apoptosis, *Cancer Res.* 58, 3495–3498.
42. Le Cam, E., Fack, F., Menissier-de Murcia, J., Cognet, J. A., Barbin, A., Sarantoglou, V., Revet, B., Delain, E., and de Murcia, G. (1994) Conformational analysis of a 139 base-pair DNA fragment containing a single-stranded break and its interaction with human poly(ADP-ribose) polymerase, *J. Mol. Biol.* 235, 1062–1071.
43. Petrucco, S., Volpi, G., Bolchi, A., Rivetti, C., and Ottonello, S. (2002) A nick-sensing DNA 3'-repair enzyme from *Arabidopsis*, *J. Biol. Chem.* 277, 23675–23683.
44. Mills, J. B., Cooper, J. P., and Hagerman, P. J. (1994) Electrophoretic evidence that single-stranded regions of one or more nucleotides dramatically increase the flexibility of DNA, *Biochemistry* 33, 1797–1803.
45. Declais, A. C., Fogg, J. M., Freeman, A. D., Coste, F., Hadden, J. M., Phillips, S. E., and Lilley, D. M. (2003) The complex between a four-way DNA junction and T7 endonuclease I, *EMBO J.* 22, 1398–1409.
46. Wojtuszewski, K., Hawkins, M. E., Cole, J. L., and Mukerji, I. (2001) HU binding to DNA: evidence for multiple complex formation and DNA bending, *Biochemistry* 40, 2588–2598.
47. Kraus, W. L., and Lis, J. T. (2003) PARP goes transcription, *Cell* 113, 677–683.
48. Rouleau, M., Aubin, R. A., and Poirier, G. G. (2004) Poly(ADP-ribose)ated chromatin domains: access granted, *J. Cell Sci.* 117, 815–825.
49. Tulin, A., and Spradling, A. (2003) Chromatin loosening by poly(ADP-ribose) polymerase (PARP) at *Drosophila* puff loci, *Science* 299, 560–562.
50. Kim, M. Y., Mauro, S., Gevry, N., Lis, J. T., and Kraus, W. L. (2004) NAD<sup>+</sup>-dependent modulation of chromatin structure and transcription by nucleosome binding properties of PARP-1, *Cell* 119, 803–814.
51. Mendoza-Alvarez, H., and Alvarez-Gonzalez, R. (2004) The 40 kDa carboxy-terminal domain of poly(ADP-ribose) polymerase-1 forms catalytically competent homo- and heterodimers in the absence of DNA, *J. Mol. Biol.* 336, 105–114.
52. Ikejima, M., Noguchi, S., Yamashita, R., Ogura, T., Sugimura, T., Gill, D. M., and Miwa, M. (1990) The zinc fingers of human poly(ADP-ribose) polymerase are differentially required for the recognition of DNA breaks and nicks and the consequent enzyme activation. Other structures recognize intact DNA, *J. Biol. Chem.* 265, 21907–21913.
53. Potaman, V. N., Shlyakhtenko, L. S., Oussatcheva, E. A., Lyubchenko, Y. L., and Soldatenkov, V. A. (2005) Specific binding of Poly(ADP-ribose) polymerase-1 to cruciform hairpins, *J. Mol. Biol.* 348, 609–615.
54. Lonskaya, I., Potaman, V. N., Shlyakhtenko, L. S., Oussatcheva, E. A., Lyubchenko, Y. L., and Soldatenkov, V. A. (2005) Regulation of poly(ADP-ribose) polymerase-1 by DNA structure-specific binding, *J. Biol. Chem.* 280, 17076–17082.

BI0507550